Energy and angular distributions of electrons emitted in proton collisions with molecular hydrogen

C. T. Plowman [1,*] I. B. Abdurakhmanov [2] I. Bray [1] and A. S. Kadyrov [1,†]

[1]*Department of Physics and Astronomy and Curtin Institute for Computation, Curtin University,*
G.P.O. Box U1987, Perth, Western Australia 6845, Australia
[2]*Pawsey Supercomputing Centre, 1 Bryce Ave, Kensington, Western Australia 6151, Australia*

The description of experimental data on energy and angular distributions of electrons produced in intermediate-energy proton collisions with H_2 has remained an insurmountable problem for over five decades. A coupled-channel method is developed that provides an accurate solution to the problem. The doubly differential cross section as a function of the energy and angle of the ejected electron is calculated. Excellent agreement between the present results and the experimental data is found. This breakthrough in theoretical modeling of differential ionization in $p + H_2$ collisions paves the way to accurate description of the recent kinematically complete experiments.

I. INTRODUCTION

Ion collisions with atoms and molecules represent one of the most fundamental physical processes and remains an active area of research [1,2]. In part this is due to an abundance of atomic collisions occurring in astrophysical and laboratory plasmas, as well as stringent accuracy requirements in hadron therapy treatment of cancer [3]. Consequently, experimentalists and theorists continue to investigate collisions between atoms and molecules to better understand the underlying physics. Researchers face unique challenges and some types of collisions that are easier to investigate in the laboratory are very difficult to calculate, and vice versa. For example, it is easier to prepare H_2 targets experimentally than H atoms [4]; however, theoretical modeling of collisions with molecules is a significantly more challenging task than those involving atomic targets. Significant differences still exist between theory and experiment for some of the most fundamental collision systems, such as proton scattering on molecular hydrogen. Recent advances in experimental techniques, e.g., cold target recoil ion momentum spectroscopy (COLTRIMS), have enabled kinematically complete experiments capable of measuring the fully differential cross sections for ionization [5] and dissociative capture [6]. Calculating the doubly and fully differential cross sections for these processes remains a challenging task for theorists. Theoretical approaches continue to be developed and applied to describe the latest highly accurate experimental data (see, e.g., Refs. [7–9] and references therein); however, the theory is still lagging far behind the experiment, particularly in the intermediate-energy region.

Recent measurements of the doubly and fully differential cross sections for ionization in $p + H_2$ collisions [10,11] reveal inconsistent agreement with the currently available theoretical results (see, for instance, Ref. [12]). In particular, significant differences between theory and experiment still

exist for the doubly differential cross section (DDCS) for ionization as a function of the emission energy and the angle of the ejected electron [13,14]. Resolving these discrepancies is an essential step towards understanding the disagreement between theory and experiment for the fully differential cross section.

The angular and energy distributions of ejected electrons were first measured by Kuyatt and Jorgensen [15] across an incident energy range from 50 to 100 keV over five decades ago. Rudd and Jorgensen [16] then measured the DDCS for ionization at 100 keV over a wider ejection energy and ejection angle range. The authors of Refs. [15,16] both found that, although the energy distribution of ejected electrons was represented reasonably by the first-order Born approximation (FBA) calculations, agreement between theory and experiment for the angular distribution was very poor. Even at an incident energy of 300 keV, where the measured total ionization cross section demonstrates improved agreement with the FBA one, significant disagreement was still observed between theory and experiment for the DDCS [17]. Additionally, when the differential cross section measured in these early experiments was integrated, the resulting total ionization cross section (TICS) was 35–100% larger than that reported by direct measurements. Toburen and Wilson [18] independently measured the DDCS for ionization in $p + H_2$ collisions from 300 keV up to 1.5 MeV. In general, their results agree well with those of Rudd *et al.* [17] at 300 keV. However, their data deviate from those of Rudd *et al.* [17] at ejection energies less than 50 eV for ejection angles greater than $30°$. The most significant difference is seen at the highest measured ejection energies and for emission in the backward direction where the cross section is very small and the signal-to-noise ratio in their measurements is low. At the larger impact energies considered by Toburen and Wilson [18], the binary-encounter peak becomes visible for ejection of high-energy electrons at small emission angles. This secondary peak in the DDCS is the result of essentially binary collisions between the projectile and the active electron.

*corey.plowman@postgrad.curtin.edu.au
†a.kadyrov@curtin.edu.au

Rudd [19] measured the DDCS for ionization at the lower impact energy of 20 keV. Here the FBA results demonstrated significant disagreement with the measurements at small ejection energies, even after considering experimental error that was greater than 20% at these ejection energies. As with their earlier data reported in Ref. [17], the integrated DDCS they measured was significantly larger than direct measurements of the TICS. Gibson and Reid [20] measured the DDCS for ionization at 50 keV for ejection energies over a range from 5 to 150 eV and emission angles from 0° to 100°; however, the TICS found by integrating their results differed from direct measurements by 33%. Furthermore, subsequent experiments called into question the accuracy of their results due to potential spreading of their proton beam [21]. The latest experimental measurements of this type were performed by Gealy *et al.* [4] using a new apparatus specifically designed to measure the flux of low-energy electrons accurately. They reported the DDCS for ionization for impact energies from 20 to 114 keV as a function of both ejection energy and angle for electron energies as small as 1.5 to 400 eV at the highest incident energy. Their angular range extended from 15° to 165°. Additionally, the integrated cross section obtained in this work agreed well with the independently measured TICS.

The experimental data of Rudd *et al.* [17] and Gibson and Reid [20] also show evidence of a sharp peak in the DDCS when the electron is emitted in the narrow forward direction. This so-called electron capture into the continuum (ECC) peak [13] is the result of the ionized electron leaving the system in the same direction and with the same velocity as the projectile. In the projectile frame this is equivalent to the electron having near-zero relative velocity. Calculating differential cross sections for ionization in this kinematic regime is a difficult problem. Accurate modeling of this interesting mechanism deserves an investigation of its own and will be addressed elsewhere. In this work, we focus on calculating the DDCS for ionization at all emission angles and energies except the forward direction.

Theoretically, the DDCS as a function of the emission energy and angle has mainly been investigated with the first Born approximation. In this approach the results for collisions with the molecular target are obtained by applying either the Bragg additivity rule or an energy-scaling procedure to the FBA results obtained for scattering on the atomic target [22]. The inability of these approaches to accurately model the underlying physics is evident from poor agreement with the experimental data of Refs. [15–18]. A different approach was taken by Macek [13] who used the first term in the Neuman expansion of Faddeev's equations for the final state of the projectile-electron-residual ion system to calculate the DDCS for ionization. The calculations were performed at an incident energy of 300 keV. The results also showed significant deviation with the experimental data. The most recent calculations of this cross section were performed by Galassi *et al.* [14] using both the FBA and the continuum-distorted-wave eikonal-initial-state (CDW-EIS) methods. As with the FBA, the CDW-EIS is a perturbative approach and only applicable at sufficiently high collision energies. Their approach to calculating the cross section for the molecular target, dubbed the continuum-distorted-wave eikonal-initial-state molecular-orbital (CDW-EIS-MO) approach, treats the target as two

independent H atoms separated by the equilibrium internuclear distance of the H_2 molecule. The cross section for proton scattering on H_2 is averaged over all orientations of the molecular target. Results are only available at four emission angles at an incident energy of 114 keV. Overall, the CDW-EIS-MO calculations demonstrate improved agreement with experiment compared to FBA calculations.

Very recently, the two-center wave-packet convergent close-coupling (WP-CCC) approach has been extended to calculate total and singly differential cross sections for all single-electron processes occurring in $p + H_2$ collisions [23,24]. This nonperturbative method accounts for strong coupling effects between different reaction channels. Previously it has been applied to calculate the DDCS as a function of the emission energy and projectile scattering angle in proton collisions with atomic hydrogen at 75 keV, demonstrating excellent agreement with experiment [25]. At this impact energy, the total ionization cross section is near its maximum and many different competing reaction channels, including electron capture by the projectile, play important roles in the collisional dynamics. For over five decades experimentalists have worked to improve the accuracy and precision of measurements of ionization cross sections in $p + H_2$ collisions [11,15,26,27], yet theorists have thus far been unable to consistently calculate the DDCS across the wide range of emission energies and angles for which experimental data are available. In this work we further develop the WP-CCC method to address this long-standing discrepancy between theory and experiment.

Unless specified otherwise, atomic units (a.u.) are used throughout this paper.

II. THEORY

The WP-CCC method is based on the semiclassical impact-parameter formalism for ion-atom scattering. The underlying approach for calculating differential cross sections for ionization in $p + H_2$ collisions is detailed in Ref. [24]. Briefly, the Schrödinger equation for the total scattering wave function Ψ_i^+, subject to the outgoing-wave boundary conditions, is $(H - E)\Psi_i^+ = 0$, where H is the full three-body Hamiltonian of the collision system and E is the total energy. The total scattering wave function develops from the initial channel i representing the projectile incident on the target in the ground electronic state. The latter is expanded in terms of N target-centered (ψ_α^T) and M projectile-centered (ψ_β^P) pseudostates,

$$\Psi_i^+ \approx \sum_{\alpha=1}^{N} F_\alpha(t, \boldsymbol{b}) \psi_\alpha^T(\boldsymbol{r}_T) e^{i\boldsymbol{q}_\alpha \cdot \boldsymbol{\rho}} + \sum_{\beta=1}^{M} G_\beta(t, \boldsymbol{b}) \psi_\beta^P(\boldsymbol{r}_P) e^{i\boldsymbol{q}_\beta \cdot \boldsymbol{\sigma}},$$

(1)

where $F_\alpha(t, \boldsymbol{b})$ and $G_\beta(t, \boldsymbol{b})$ are expansion coefficients that depend on time t and impact parameter $\boldsymbol{b}$. We position the origin of our coordinate system at the target nucleus and use two sets of Jacobi coordinates. In the first set, $\boldsymbol{r}_T$ is the position vector of the active electron relative to the target nucleus and $\boldsymbol{\rho}$ is the position of the projectile nucleus relative to the target system. In the second set, $\boldsymbol{r}_P$ is the position of the active electron relative to the projectile and $\boldsymbol{\sigma}$ is the position of the atom

formed by the projectile after capturing the electron (hereafter called the projectile atom) relative to the residual target ion, H_2^+. The momentum of the projectile relative to the target is denoted $\boldsymbol{q}_\alpha$ and the momentum of the projectile atom relative to the target nucleus is denoted $\boldsymbol{q}_\beta$. The projectile moves with the velocity $\boldsymbol{v}$ in a straight line parallel to the z axis with its position given by $\boldsymbol{R} = \boldsymbol{b} + \boldsymbol{v}t$, where the impact parameter is perpendicular to the projectile velocity, $\boldsymbol{b} \cdot \boldsymbol{v} = 0$. We include both target- and projectile-centered basis states in Eq. (1) to accurately calculate ionization since the positive charge of the projectile results in a high probability of ejected electrons leaving the system in the vicinity of the projectile nucleus. This electron capture into the continuum process contributes significantly to the total ionization cross section [28].

In order to describe the structure of the H_2 molecule, we use the effective one-electron method suggested by Vanne and Saenz [29]. In this method the field of the residual target ion is collectively represented using a model potential that results in an accurate ground-state ionization energy of H_2 corresponding to the equilibrium internuclear separation. The radial wave functions of the negative-energy target states in Eq. (1) are constructed by solving the Schrödinger equation for the target using an iterative Numerov approach. The energies of the states are given by the corresponding eigenvalues. To construct pseudostates representing the continuum, the continuum is subdivided into N_c nonoverlapping momentum intervals from $\kappa_{\min}$ to $\kappa_{\max}$. We then construct a wave packet for each interval by numerically integrating the continuum wave over the width of the interval. The corresponding energy of the continuum pseudostate is given by the midpoint of the interval. The procedure is repeated for all N_c intervals. We find that $\kappa_{\max} = 10$ a.u. is sufficiently large for the results of interest to converge. Combined, the set of negative- and positive-energy pseudostates form an orthonormal basis that diagonalizes the target Hamiltonian. The projectile-atom states are constructed from eigenstates of the hydrogen atom and wave packets made using the pure Coulomb wave function. Together they also form an orthonormal basis that spans the negative- and positive-energy spectrum of the projectile atom.

The expansion of the total scattering wave function in Eq. (1) is substituted into the time-independent Schrödinger equation. Using the semiclassical approximation, after some algebra, this results in a set of first-order differential equations for the unknown expansion coefficients. In the limit as $t \to +\infty$ the expansion coefficients $F_\alpha(t, \boldsymbol{b})$ and $G_\beta(t, \boldsymbol{b})$ yield the scattering amplitudes for the final channel specified by α and β, respectively. See Refs. [23,24] for details of the scattering equations and matrix elements.

Once the expansion coefficients have been calculated, the momentum-space transition amplitudes corresponding to direct scattering, $T_{fi}^{\mathrm{DS}}(\boldsymbol{q}_f, \boldsymbol{q}_i)$, and electron capture, $T_{fi}^{\mathrm{EC}}(\boldsymbol{q}_f, \boldsymbol{q}_i)$, are calculated using the Fourier-Bessel transformations of $F_f(+\infty, \boldsymbol{b})$ and $G_f(+\infty, \boldsymbol{b})$, respectively. The WP-CCC approach to calculating differential ionization cross sections is detailed in Ref. [24]. Briefly, we construct identity operators from our complete sets of target and projectile pseudostates and then insert these into the general definition of the scattering amplitude given in Refs. [30,31]. This splits the total ionization amplitude into two parts, one for direct ionization

of the target and one for electron capture into the continuum of the projectile. The direct-ionization (DI) amplitude is given by the product of the direct-scattering amplitudes of positive-energy pseudostates and the overlap between the corresponding pseudostate and true continuum wave,

$$T_{fi}^{\mathrm{DI}}(\boldsymbol{\kappa}, \boldsymbol{q}_f, \boldsymbol{q}_i) = \frac{1}{(2\pi)^{3/2}} \sum_{\ell m} \langle \varphi_{\boldsymbol{\kappa}}^{\mathrm{T}} | \psi_f^{\mathrm{T}} \rangle T_{fi}^{\mathrm{DS}}(\boldsymbol{q}_f, \boldsymbol{q}_i), \quad (2)$$

where $\boldsymbol{\kappa}$ is the momentum of the ionized electron in the target-centered coordinate system and $\varphi_{\boldsymbol{\kappa}}^{\mathrm{T}}$ is the true continuum wave solution of the target residual ion obtained using the effective potential. The ECC amplitude is given by the product of the amplitudes for electron capture into positive-energy pseudostates and the overlap between the corresponding pseudostate and pure Coulomb wave,

$$T_{fi}^{\mathrm{ECC}}(\boldsymbol{\varkappa}, \boldsymbol{q}_f, \boldsymbol{q}_i) = \frac{1}{(2\pi)^{3/2}} \sum_{\ell m} \langle \varphi_{\boldsymbol{\varkappa}}^{\mathrm{P}} | \psi_f^{\mathrm{P}} \rangle T_{fi}^{\mathrm{EC}}(\boldsymbol{q}_f, \boldsymbol{q}_i), \quad (3)$$

where $\boldsymbol{\varkappa}$ is the momentum of the ionized electron in the projectile-centered coordinate system and $\varphi_{\boldsymbol{\varkappa}}^{\mathrm{P}}$ is the pure Coulomb wave. However, the DI and ECC amplitudes are given in the target- and projectile-centered frames of reference, respectively. Hence, we must bring the amplitudes into a common frame. We choose the laboratory frame of reference, where the target is at rest, in order to compare our results with experimental data. Thus, only the ECC component needs to be transformed. Then, the fully differential cross section (FDCS) for ionization is calculated according to

$$\frac{d^3\sigma}{dE_e d\Omega_e d\Omega_f} = \frac{\mu_{\mathrm{T}}^2}{(2\pi)^2} \frac{q_f \kappa_n}{q_i} \left(\left| T_{fi}^{\mathrm{DI}}(\boldsymbol{q}_f, \boldsymbol{q}_i, \boldsymbol{\kappa}_n) \right|^2 \right.$$
$$\left. + \left| T_{fi}^{\mathrm{ECC}}(\boldsymbol{q}_f, \boldsymbol{q}_i, \boldsymbol{\kappa}_n - \boldsymbol{v}) \right|^2 \right), \quad (4)$$

where μ_{T} is the reduced mass of the $p + H_2$ system and $\boldsymbol{\kappa}_n$ is the momentum of the wave packet that represents the nth continuum bin. Thus, in our approach the FDCS has two parts, the DI and ECC ones, that are added incoherently. Our earlier calculations for proton-induced ionization of atomic hydrogen showed that, when the basis size is sufficiently large, the coherent and incoherent combinations of the DI and ECC amplitudes lead to practically the same cross sections [25]. It was concluded that for practical purposes of calculating the differential ionization cross sections, both ways could be used. Therefore, we use the incoherent combination since it requires significantly less CPU time and resources. It also makes transparent the unitarity of the close-coupling formalism.

The DI component of the DDCS for ionization resulting in electron emission along the surface of a cone at an angle of θ_e to the z axis with a momentum between the boundaries of the nth continuum bin is found by analytically integrating over the scattering angle of the projectile. This leads to

$$\frac{d^2\sigma^{\mathrm{DI}}}{dE_e d\Omega_e} = \frac{2\pi}{\kappa_n w_n} \sum_{\ell=0}^{\ell_{\max}} \sum_{\ell'=0}^{\ell'_{\max}} \sum_{m=-\ell}^{\ell}$$
$$\times Y_{\ell m}^*(\hat{\boldsymbol{\kappa}}_n) Y_{\ell' m}(\hat{\boldsymbol{\kappa}}_n)(-i)^{\ell'-\ell} e^{i(\sigma_{\ell'} - \sigma_\ell)}$$
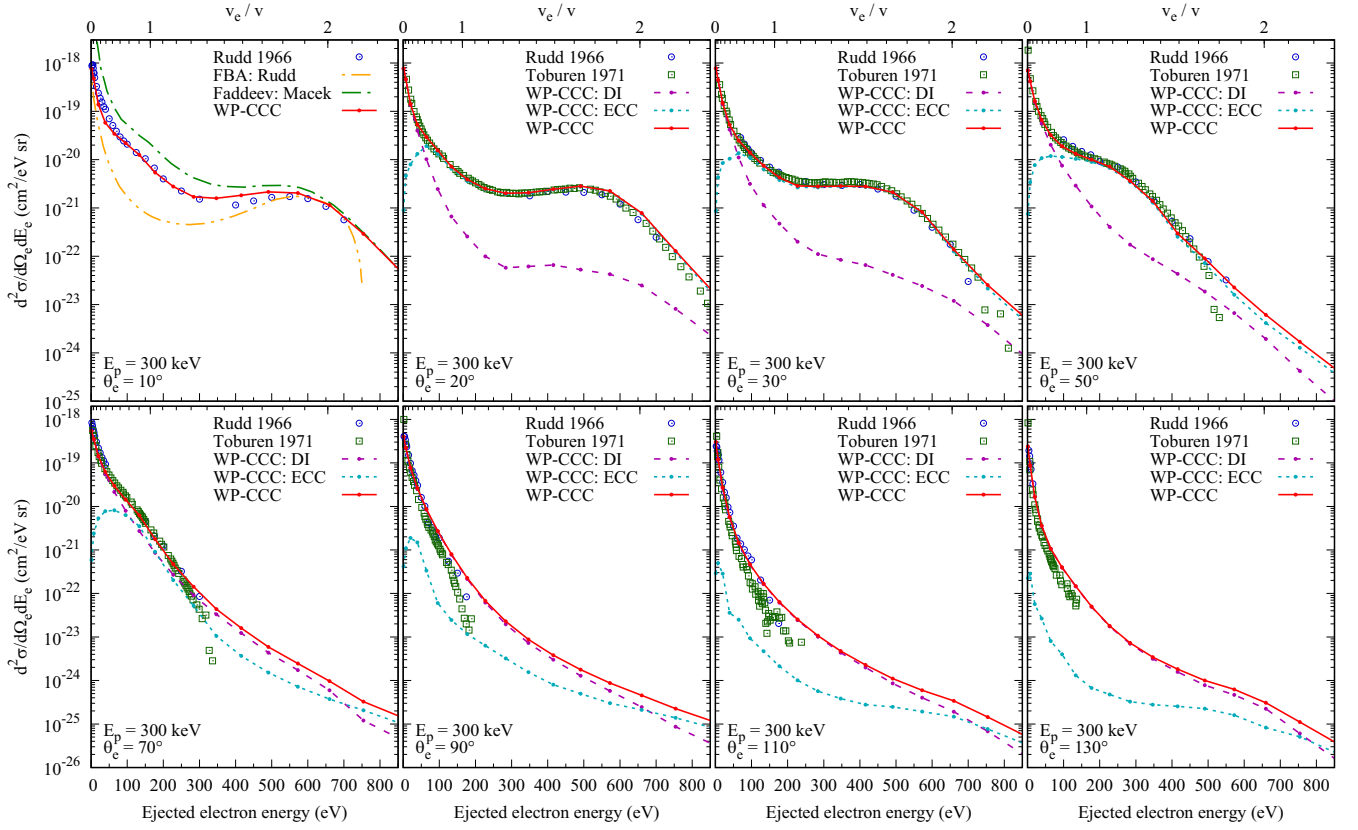$$\times \int db \, b \, \tilde{F}_{n\ell m}^*(\infty, b) \tilde{F}_{n\ell' m}(\infty, b), \quad (5)$$

FIG. 1. Doubly differential cross section of ionization for 300-keV proton collisions with H_2 as a function of the ejected electron energy at various emission angles. Experimental data are from Rudd *et al.* [17] and Toburen and Wilson [18]. Theoretical results: The WP-CCC approach, the first-order Born approximation by Rudd *et al.* [17], and the Faddeev approach by Macek [13]. The present DI and ECC components are also shown.

where $\tilde{F}_{nlm}(t, b) = e^{im\phi_b} F_{nlm}(t, \boldsymbol{b})$ is the target-centered expansion coefficient that does not depend on the azimuthal angle of the impact parameter. For the ECC component we follow the same procedure. Therefore, the ECC part of the DDCS has the same form as the DI component in Eq. (5), but with the substitutions $\varkappa \to \kappa - \boldsymbol{v}$, and $\tilde{F}_{nlm} \to \tilde{G}_{nlm}$, where $\tilde{G}_{nlm}(t, b) = e^{im\phi_b} G_{nlm}(t, \boldsymbol{b})$ is the projectile-centered expansion coefficient that does not depend on the azimuthal angle of the impact parameter.

We find that a basis containing $10 - \ell$ bound states for each included orbital quantum number ℓ up to $\ell_{max} = 4$ is sufficient to obtain converged results. The continuum was discretized with 25 bins for each included orbital quantum number and the electron-momentum cutoff was 10.0 a.u. The z grid was extended from -200 to $+200$ a.u.

III. RESULTS

We have calculated the DDCS in the incident energy range spanning from 20 to 300 keV, which represents the most difficult intermediate-energy region where the total ionization cross section peaks and where many competing reaction channels play important roles in the collisional dynamics. Here we show our results at a representative collision energy. The further details of the calculations and more results will be reported elsewhere. Figure 1 shows the present results for

the DDCS for ionization at an incident energy of 300 keV as a function of the ejected electron energy for emission angles from $10°$ to $130°$. We can compare our calculations to the two independent sets of experimental data from Rudd *et al.* [17] and Toburen and Wilson [18]. Additionally, we also show the DI and ECC components of the cross section, except at $10°$ where we compare with the FBA calculations from Rudd *et al.* [17] and the calculations based on the Faddeev equations by Macek [13]. There are no other calculations for other emission angles.

At the top of each panel we show the velocity of the ejected electron v_e in terms of the projectile velocity. In the forward direction the ECC component peaks when $v_e/v = 1$. The smallest emission angle considered here is $10°$. We see no evidence of the ECC peak in our result or the experimental data at this emission angle.

We find excellent agreement between our calculations and the experimental data of Rudd *et al.* [17]. The present results agree well with the measurements of Toburen and Wilson [18] as well, but only within the energy range where their data are in agreement with the data of Rudd *et al.* [17]. For emission into $10°$ the FBA calculations by Rudd *et al.* [17] significantly deviate from the experimental results, underestimating the data from 0 up to 600 eV and then falling off sharply at higher emission angles. At this impact energy, the projectile velocity is $v = 3.465$ a.u. It is sufficiently high for the FBA

to be considered suitable for calculating the TICS. However, we see that the FBA fails to reproduce the underlying DDCS. The approach used by Macek [13] based on the Faddeev equations overestimates the experimental data significantly at small emission energies and then decreases to eventually agree at 650 and 700 eV.

The WP-CCC results reproduce both the main peak in the DDCS for the very low emission energies and the binary-encounter peak. Furthermore, we explicitly calculated the direct ionization and electron capture into the continuum contributions to the DDCS. This allows us to analyze the roles these mechanisms play in emission of electrons in a wide range of kinematic regimes. We find that for small ejection angles the DDCS is dominated by DI for small energies and ECC for larger ejection energies. Near the emission angle of $70°$, the DI and ECC components become comparable, except for very small ejection energies where the ECC part falls off steeply towards the ionization threshold. At $90°$ and above, the DDCS is primarily made of DI, only for very large ejection energies does the ECC contribute for backward ejection angles. This makes physical sense since ejection into angles greater than $90°$ will result in the electron being closer to the target nucleus while the projectile nucleus moves away from the scattering system in the forward direction.

IV. CONCLUSIONS AND SUMMARY

The present results represent the first calculations of the DDCS for $p + H_2$ collisions in the intermediate-energy range, in particular, at 300 keV, that are capable of reproducing the available experimental data. The previously applied theoretical approaches are perturbative and hence are only applicable at sufficiently high projectile energies. Their fundamental assumptions are not valid when the projectile velocity is comparable to or less than the orbital velocity of the target electrons. The WP-CCC method is the only nonperturbative approach to differential ionization that accounts for the strong coupling between the reaction channels. Additionally, we are able to distinguish between the DI and ECC mechanisms, providing further insight into the underlying physics. The present results demonstrate that strong coupling between reaction channels and both DI and ECC mechanisms play important roles in the electron emission cross section, indicating that inclusion of the two-center nature of the scattering system is essential for accurately calculating differential cross sections for ionization.

This work lays the foundations for applying the WP-CCC approach to other types of DDCS for ionization, such as those differential in both the scattering angle of the projectile and the ejected electron energy, which were measured in Refs. [32,33]. Currently there is no theory capable of accurately describing the ionization cross-section differential in both the scattering angle of the projectile and the ejected electron energy across the energy range of the emitted electrons measured by experiment. The current results represent an essential step towards developing a single complete theory capable of describing the different types of DDCS in all kinematic regimes. It is worth mentioning that the WP-CCC approach has recently been used to calculate singly differential cross sections for ionization in $p + He$ collisions, also resulting in very good agreement with the experimental data [34]. Moreover, calculations of the FDCS for ionization in energetic proton-helium collisions using the single-center WP-CCC method [7,8] showed very good agreement with the recent high-resolution experiment by Gassert *et al.* [5]. Very recent results based on a parabolic quasi-Sturmian approach to ionization in $p + He$ collisions by Zaytsev *et al.* [9] also show good agreement with the experimental data from Ref. [5]. However, both theoretical approaches predict a shift in the position of the binary peak. Furthermore, there is currently no theory that can describe the experimental data for the FDCS at 75 keV measured by Schulz *et al.* [35] and Dhital *et al.* [11] consistently in all kinematic regimes. Therefore, we intend to apply the two-center WP-CCC method to calculate the FDCS in proton collisions with He and H_2 to determine if higher-order effects resulting from the presence of the second center are able to explain the aforementioned discrepancies. The recent fully differential study of capture with vibrational dissociation in $p + H_2$ collisions [6,36] is another intriguing problem that presently available methods cannot describe. We are working on extending our method to this problem.

The H_2 molecule is a two-center target. In principle, the waves scattered from the two centers may interfere. One can expect that this may affect the cross sections. However, the experimental data of Rudd *et al.* [17] and Toburen and Wilson [18] for the DDCS in the energy and angle of the ejected electron at a projectile energy of 300 keV, investigated here, show no evidence of interference. This can be seen in Fig. 1. Nevertheless, experiments by Hossain *et al.* [37] and Stolterfoht *et al.* [38] suggest that interference becomes important at significantly higher projectile energies and for highly charged ions. At the same time, interference could also be important for the DDCS in the energy of the electron and the scattering angle of the projectile, and for fully differential cross sections. We will investigate these elsewhere.

In conclusion, we have developed an approach to differential ionization in proton collisions with molecular hydrogen. The method has been applied to calculate the energy and angular distributions of emitted electrons. The approach provides an accurate description of the experimental data, resolving a long-standing theoretical challenge. This is an essential step towards closing the gap between theory and the latest experimental developments.

[1] M. Schulz, Editor, *Ion-Atom Collisions: The Few-Body Problem in Dynamic Systems* (De Gruyter, Berlin, 2019).

[2] Dž. Belkić, I. Bray, and A. Kadyrov (Eds.), *State-of-the-Art Reviews on Energetic Ion-Atom and Ion-Molecule Collisions* (World Scientific, Singapore, 2019).

[3] I. Abril, R. Garcia-Molina, P. de Vera, I. Kyriakou, and D. Emfietzoglou, Adv. Quantum Chem. **65**, 129 (2013).

[4] M. W. Gealy, G. W. Kerby, Y.-Y. Hsu, and M. E. Rudd, Phys. Rev. A **51**, 2247 (1995).

[5] H. Gassert, O. Chuluunbaatar, M. Waitz, F. Trinter, H.-K. Kim, T. Bauer, A. Laucke, C. Müller, J. Voigtsberger, M. Weller *et al.*, Phys. Rev. Lett. **116**, 073201 (2016).

[6] B. R. Lamichhane, T. Arthanayaka, J. Remolina, A. Hasan, M. F. Ciappina, F. Navarrete, R. O. Barrachina, R. A. Lomsadze, and M. Schulz, Phys. Rev. Lett. **119**, 083402 (2017).

[7] I. B. Abdurakhmanov, A. S. Kadyrov, I. Bray, and K. Bartschat, Phys. Rev. A **96**, 022702 (2017).

[8] I. B. Abdurakhmanov, A. S. Kadyrov, S. U. Alladustov, I. Bray, and K. Bartschat, Phys. Rev. A **100**, 062708 (2019).

[9] A. S. Zaytsev, D. S. Zaytseva, S. A. Zaytsev, L. U. Ancarani, and K. A. Kouzakov, Phys. Rev. A **105**, 062818 (2022).

[10] A. Hasan, T. Arthanayaka, B. Lamichhane, S. Sharma, S. Gurung, J. Remolina, S. Akula, D. H. Madison, M. F. Ciappina, R. D. Rivarola *et al.*, J. Phys. B: At., Mol. Opt. Phys. **49**, 04LT01 (2016).

[11] M. Dhital, S. Bastola, A. Silvus, J. Davis, B. R. Lamichhane, E. Ali, M. F. Ciappina, R. Lomsadze, A. Hasan, D. H. Madison, and M. Schulz, Phys. Rev. A **102**, 032818 (2020).

[12] A. Igarashi and L. Gulyás, J. Phys. B: At., Mol. Opt. Phys. **51**, 035201 (2018).

[13] J. Macek, Phys. Rev. A **1**, 235 (1970).

[14] M. E. Galassi, R. D. Rivarola, and P. D. Fainstein, Phys. Rev. A **70**, 032721 (2004).

[15] C. E. Kuyatt and T. Jorgensen, Phys. Rev. **130**, 1444 (1963).

[16] M. E. Rudd and T. Jorgensen, Phys. Rev. **131**, 666 (1963).

[17] M. E. Rudd, C. A. Sautter, and C. L. Bailey, Phys. Rev. **151**, 20 (1966).

[18] L. H. Toburen and W. E. Wilson, Phys. Rev. A **5**, 247 (1972).

[19] M. E. Rudd, Phys. Rev. A **20**, 787 (1979).

[20] D. K. Gibson and I. D. Reid, Double Differential Cross Sections for Electrons Ejected from H_2, O_2, N_2, CO_2, CH_4, H_2O and Ar by 50 keV Protons, Report AAEC/E659 (Australian Atomic Energy Commission, Lucas Heights, NSW, 1987), http://apo.ansto.gov.au/dspace/handle/10238/821.

[21] W.-Q. Cheng, M. E. Rudd, and Y.-Y. Hsu, Phys. Rev. A **40**, 3599 (1989).

[22] D. R. Bates and G. W. Griffing, Proc. Phys. Soc. A **66**, 961 (1953).

[23] C. T. Plowman, I. B. Abdurakhmanov, I. Bray, and A. S. Kadyrov, Eur. Phys. J. D **76**, 31 (2022).

[24] C. T. Plowman, I. B. Abdurakhmanov, I. Bray, and A. S. Kadyrov, Eur. Phys. J. D **76**, 129 (2022).

[25] I. B. Abdurakhmanov, J. J. Bailey, A. S. Kadyrov, and I. Bray, Phys. Rev. A **97**, 032707 (2018).

[26] M. Rudd, Y. Kim, D. Madison, and J. Gallagher, Rev. Mod. Phys. **57**, 965 (1985).

[27] M. E. Rudd, Y. K. Kim, D. H. Madison, and T. J. Gay, Rev. Mod. Phys. **64**, 441 (1992).

[28] C. T. Plowman, K. H. Spicer, I. B. Abdurakhmanov, A. S. Kadyrov, and I. Bray, Phys. Rev. A **102**, 052810 (2020).

[29] Y. V. Vanne and A. Saenz, J. Mod. Opt. **55**, 2665 (2008).

[30] A. S. Kadyrov, I. Bray, A. M. Mukhamedzhanov, and A. T. Stelbovics, Phys. Rev. Lett. **101**, 230405 (2008).

[31] A. S. Kadyrov, I. Bray, A. M. Mukhamedzhanov, and A. T. Stelbovics, Ann. Phys. **324**, 1516 (2009).

[32] J. S. Alexander, A. C. Laforge, A. Hasan, Z. S. Machavariani, M. F. Ciappina, R. D. Rivarola, D. H. Madison, and M. Schulz, Phys. Rev. A **78**, 060701(R) (2008).

[33] S. Sharma, T. P. Arthanayaka, A. Hasan, B. R. Lamichhane, J. Remolina, A. Smith, and M. Schulz, Phys. Rev. A **89**, 052703 (2014).

[34] K. H. Spicer, C. T. Plowman, I. B. Abdurakhmanov, S. U. Alladustov, I. Bray, and A. S. Kadyrov, Phys. Rev. A **104**, 052815 (2021).

[35] M. Schulz, A. Hasan, N. V. Maydanyuk, M. Foster, B. Tooke, and D. H. Madison, Phys. Rev. A **73**, 062704 (2006).

[36] S. Bastola, M. Dhital, B. Lamichhane, A. Silvus, R. Lomsadze, J. Davis, A. Hasan, A. Igarashi, and M. Schulz, Phys. Rev. A **105**, 032805 (2022).

[37] S. Hossain, A. Alnaser, A. Landers, D. Pole, H. Knutson, A. Robison, B. Stamper, N. Stolterfoht, and J. Tanis, Nucl. Instrum. Methods Phys. Res., Sect. B **205**, 484 (2003).

[38] N. Stolterfoht, B. Sulik, V. Hoffmann, B. Skogvall, J. Y. Chesnel, J. Rangama, F. Frémont, D. Hennecart, A. Cassimi, X. Husson, A. L. Landers, J. A. Tanis, M. E. Galassi, and R. D. Rivarola, Phys. Rev. Lett. **87**, 023201 (2001).